BASIC SCIENCE

Nanomedicine: Nanotechnology, Biology, and Medicine
10 (2014) 1453–1463

Original Article

nanomedjournal.com

Protein corona composition does not accurately predict hematocompatibility of colloidal gold nanoparticles

Marina A. Dobrovolskaia, PhD[a,*], Barry W. Neun, BS[a], Sonny Man, MS[a], Xiaoying Ye, PhD[b], Matthew Hansen, MS[a], Anil K. Patri, PhD[a], Rachael M. Crist, PhD[a], Scott E. McNeil, PhD[a]

[a]*Nanotechnology Characterization Laboratory, Frederick National Laboratory for Cancer Research, Leidos Biomedical Research Inc., Frederick, Maryland*
[b]*Laboratory of Proteomics and Analytical Technology, Cancer Research Technology Program, Frederick National Laboratory for Cancer Research, Leidos Biomedical Research Inc., Frederick, Maryland*

Received 23 October 2013; accepted 25 January 2014

Abstract

Proteins bound to nanoparticle surfaces are known to affect particle clearance by influencing immune cell uptake and distribution to the organs of the mononuclear phagocytic system. The composition of the protein corona has been described for several types of nanomaterials, but the role of the corona in nanoparticle biocompatibility is not well established. In this study we investigate the role of nanoparticle surface properties (PEGylation) and incubation times on the protein coronas of colloidal gold nanoparticles. While neither incubation time nor PEG molecular weight affected the specific proteins in the protein corona, the total amount of protein binding was governed by the molecular weight of PEG coating. Furthermore, the composition of the protein corona did not correlate with nanoparticle hematocompatibility. Specialized hematological tests should be used to deduce nanoparticle hematotoxicity.

From the Clinical Editor: It is overall unclear how the protein corona associated with colloidal gold nanoparticles may influence hematotoxicity. This study warns that PEGylation itself may be insufficient, because composition of the protein corona does not directly correlate with nanoparticle hematocompatibility. The authors suggest that specialized hematological tests must be used to deduce nanoparticle hematotoxicity.

Key words: Nanoparticles; Protein corona; Complement; Coagulation; Hematocompatibility

Increasing use of nanotechnology in biology and medicine accentuates the importance of understanding nanomaterial interactions with cells and biological fluids. Nanoparticle safety and effective performance as drug-delivery platforms are influenced by their disposition and clearance in the body. The latter is determined by nanoparticle physicochemical properties such as size, charge, hydrophobicity and shape.[1,2] Proteins bind to a nanoparticle surface almost immediately upon entry into the blood stream. Some of these proteins stay on the surface as long as particles circulate in the blood stream and "target" the particle to certain cells and tissues. For example, ApoE binding to the surface of polysorbate 80 coated nanoparticles is believed to deliver these particles to the brain, while fetuin is thought to "mark" the particle for macrophage uptake through a specific scavenger-receptor mediated route.[3–6] Protein binding affects nanoparticle hydrodynamic size and charge[7] and thus may influence the way cells and tissues interact with and process the particles, ultimately guiding cellular uptake, clearance route and organ accumulation. Recent studies have also demonstrated that proteins adsorbed onto a nanoparticle's surface change after cellular uptake and intracellular distribution.[8]

The human blood plasma protein repertoire is very dynamic and is sensitive to physiological changes. The reason(s) why some proteins are present in plasma permanently and others reside there only temporarily can be manifold. For example, some proteins are present in plasma only during infection or stress (e.g. C reactive protein). Other proteins are always present, but levels can fluctuate depending on diet (e.g. lipoproteins), infection (e.g. cytokines), or stress (e.g. serum deprivation protein, heat shock proteins). Also, some "housekeeping" protein levels (e.g. albumin, globulin, and fibrinogen) fluctuate in response to environmental changes, while a variety of other proteins (e.g. blood group antigens, Rhesus factor) are

Conflict of Interest: The study was supported in whole or in part by federal funds from the National Cancer Institute, National Institutes of Health, under contract HHSN261200800001E. The content of this publication does not necessarily reflect the views or policies of the Department of Health and Human Services, nor does mention of trade names, commercial products, or organizations imply endorsement by the U. S. Government.

*Corresponding author.
E-mail address: marina@mail.nih.gov (M.A. Dobrovolskaia).

http://dx.doi.org/10.1016/j.nano.2014.01.009
1549-9634/

only present in the blood of individuals with certain genetic backgrounds. In addition, infections and diseases, contribute foreign and aberrant proteins, which otherwise are not present in plasma. Consequently, even when using blood from healthy donor volunteers, the composition of plasma proteins can vary greatly between individuals. Intuitively, these facts suggest that in order to link protein corona composition to nanoparticle toxicity one would have to study the corona for each individual patient at a given time. The complexity of such an approach is further convoluted by the fact that phlebotomy, blood handling and storage conditions of plasma can also affect the protein repertoire.

Formation of protein corona is also a dynamic process, however opinions about the mechanism of protein binding diverge.[9–13] While some studies clinch in favor of protein displacement,[9,13] others conclude there is no typical Vroman effect in nanoparticle-protein interaction.[12] Moreover, a range of opinions exist regarding the role plasma protein binding plays in defining the toxicity of nanoparticles.[14–20] The differences in conclusions between these studies are not surprising because nanoparticles (gold colloids, silver colloids, iron oxides, polystyrene and acrylamide), the source of protein (human plasma, culture medium containing diluted fetal bovine serum, isolated individual proteins), and methods of analysis (gel-electrophoresis, mass spectrometry, fluorescent correlation spectroscopy, or a combination thereof) widely vary between studies. Therefore, questions about composition and dynamics of the protein corona and its role in nanoparticle biocompatibility still require careful examination.

Colloidal gold particles are considered a versatile biomedical platform. Their applications include image enhancing contrast agents, biosensors and drug-delivery vehicles.[21–24] Although experimental use of colloidal gold *in vivo* was described in the early 1970s, the main apprehension for their clinical *in vivo* application is rapid particle clearance from the blood stream and accumulation in organs of the mononuclear phagocytic system (MPS).[21,25–28] To prolong particle circulation and eliminate potential long term toxicity, surface modification of colloidal gold with hydrophilic polymers such as poly(ethylene glycol) (PEG) has proven a reliable shield, provided these coatings are stable and not displaced by proteins in the blood stream.

Previously it has been shown that colloidal gold particles adsorb serum proteins and that protein binding influences their clearance by immune cells.[25] Paciotti et al reported that 30 nm gold colloids rapidly accumulate in the liver and spleen, while their 20 kDa PEG-functionalized counterparts remained in circulation, allowing these particles to effectively deliver drugs into tumor tissue.[23] The molecular identity of proteins bound to the surface of anionic colloidal gold nanoparticles has been reported[7]; however, the role of incubation time and PEG surface coating on the formation and composition of the protein corona has not been explored.

In the present study we used 30 nm citrate stabilized gold nanoparticles from a commercial source to prepare several formulations bearing PEG of various molecular weights (2 kDa, 5 kDa, 10 kDa and 20 kDa). These PEG coatings were selected because of their common use in nanomedicines involving gold colloids and gold nanoshells.[23,29,30] Both uncoated and PEGylated particles were incubated with pooled human plasma for various time periods: 5 min, 30 min, 1 h, 6 h and 24 h. The amount of bound protein, as well as the composition of the protein corona, was then studied by mass spectrometry. The most abundant proteins in the corona were fibrinogen and complement, central in plasma coagulation and complement activation, respectively; therefore, we also performed *in vitro* biological assessments to ascertain whether nanoparticle binding to these proteins would alter their function.

Table 1
Physicochemical characterization of gold colloids.

Nanoparticles	DLS (intensity-peak) (nm)	Zeta potential (mV)	[Au] by ICP-MS (μg/mL)
30 nm	35.1 ± 0.3	−30.4 ± 2.0	42.02 ± 4.35
30 nm + 2 kDa PEG	58.5 ± 0.7	−8.7 ± 0.8	80.87 ± 3.86
30 nm + 5 kDa PEG	74.5 ± 0.9	−7.9 ± 0.5	60.68 ± 2.96
30 nm + 10 kDa PEG	83.9 ± 1.1	−6.7 ± 1.2	78.30 ± 3.56
30 nm + 20 kDa PEG	107 ± 1.1	−6.0 ± 1.1	91.07 ± 4.32

Nanoparticle hydrodynamic size, charge and concentration of gold was measured by dynamic light scattering, zeta potential analyzer and ICM-MS, respectively, as described in materials and methods. Shown is mean result ± standard deviation (N = 12).

Methods

Reagents

Colloidal gold nanoparticles were purchased from TedPella (Redding, CA, USA). Cobra venom factor and veronal buffer were purchased from Quidel Corporation (San Diego, CA, USA) and Boston Bioproducts (Boston, MA, US), respectively. Normal and abnormal coagulation controls, buffers, and activators for coagulation assays were purchased from Diagnostica Stago (Parsippany, NJ, USA).

Synthesis of PEGylated gold colloids

MethoxyPEG gold nanoparticles were synthesized following a modified procedure by Mirkin et al.[31] Procedural details are outlined in the Supplemental Section.

Research donor blood

Healthy human volunteer blood specimens were drawn under NCI-Frederick Protocol OH99-C-N046. Details about sample handling and processing are provided in supplemental materials.

Protein binding

Gold nanoparticles were used at equivalent gold concentrations. To achieve this, PEGylated gold nanoparticles were diluted to a final concentration of 42 μg of gold per mL, i.e. the lowest concentration of all test samples. Next, 250 μL of each stock solution (10.5 μg of gold) was placed into sterile, pyrogen-free, low-retention eppendorf tubes, and the volume was adjusted

Table 2
Individual proteins in the protein corona.

Protein category	Inter-assay variability		Intra-assay variability	
	Experiment 1	Experiment 2	Experiment 3A	Experiment 3B
Cell adhesion	Fibronectin, vitronectin, thrombospondin	Fibronectin, vitronectin, thrombospondin, integrins, beta parvin, vasodilator-stimulated phosphoprotein	fibronectin	fibronectin
Complement	C1q, C1r, C1s, C4a, C4b, C5, C8, C9, B, H	C1q, C3, C4a	C1q, C1r, C1s, C4a, C4b, C3, H	C1q, C1r, C1s, C4a, C4b, C3, H
Coagulation	Fibrinogen, vWF, FXII, plasminogen, antithrombin, PF4, plekstrin, pGP, CD9, histidine-rich glycoprotein	Fibrinogen, FXIII, pGP, kininogen, CD9, histidine-rich glycoprotein, multimerin	Fibrinogen, FXII, vit K dependent protein	Fibrinogen, FXII, vit K dependent protein
Immunoglobulins	IgG and IgM light chains	IgG and IgM light chains	IgG and IgM light chains	IgG and IgM light chains
Cytoskeleton	Actin, myosin, tubulin, gelsolin, filamin, talin	Actin, myosin, tropomyosin, tubulin, filamin, gelsolin, F-actin, vinculin, coronin, cofilin, transgelin, ezrin, zyxin, profiling, caldesmon, PDZ and LIM domain protein 1, multimerin	Actin, myosin, gelsolin, talin	Actin, myosin, gelsolin, talin
Transport	Hemoglobin, albumin, anion transport protein	Albumin, anion transport protein, Apo C, Apo E, Apo A, Apo J, hemoglobin, 78kD glucose regulated protein	Hemoglobin, hemopexin, serum amyloid A	Hemoglobin, hemopexin, serum amyloid A
Extracellular matrix	EMP, hyaluronan	Tenascin	ND	EMP
Cellular signal transduction	ND	Ras, Rab, 14-3-3 protein Z, protein S100-A9, fermitin	ND	ND
Enzymes	ND	Glyceraldehyde phosphate dehydrogenase, adenylyl cyclase, aldolase, isocitrate dehydrogenase, protein-disulfide isomerase, triosephosphate isomerase, ATP synthase, lactade dehydrogenase, enolase, pyruvate kinase, frusctose-biphosphate aldolase, peptidyl-prolyl cis-trans isomerase, carbonic anhydrase, glyceraldehyde-3 phosphate dehydrogenase	ND	ND
Stress-response	ND	Heat shock protein, serum-deprivation protein	ND	ND
Other	LBP, serum amyloid P, secreted phosphoprotein 24, erythrocyte band 7 integral membrane protein, pigment epithelium derived factor, plasma protease C1 inhibitor, histone H2B and H4, glyceraldehyde-3-phosphate dehydrogenase, estrogen receptor	Histone H4, Hermansky-Pudlock syndrome 1 protein, thymosin, erythrocyte band 7 inhegral membrane protein	Estrogen receptor, α2-macroglobulin	Estrogen receptor

30 nm colloidal gold nanoparticles were incubated with pooled human plasma and proteins in the corona were identified by mass spectrometry. Presented is the summary of all proteins identified over 5 min, 30 min, 1 h, 6 h and 24 h incubations, grouped by their function. ND, none detected.

to 1 mL with sterile water. Pooled human plasma (1 mL) was then added to each tube and samples were incubated on a rotary mixer for 5 min, 30 min, 1 h, 6 h and 24 h at 37 °C. Following incubation, the tubes were centrifuged 10 min at 4 °C in a microcentrifuge. The pellets were washed 3 times with 2 mL of sterile PBS and the final pellets were processed for analysis by mass spectrometry. Water (1 mL) was used as a control for non-specific adherence of proteins to the tubes.

Mass spectrometry

Particles with bound proteins were treated with trypsin prior to mass spectrometry analysis. Trypsinized samples were analyzed by a nano-ESI reversed-phase liquid chromatography using an Agilent 1100 nano-flow LC system (Agilent Technologies, Inc., Santa Clara, CA, USA) coupled online to a LTQ Orbitrap XL mass spectrometer (Thermo Fisher Scientific, Waltham, MA, USA). Detailed protocol is provided in supplementary materials section.

Data analysis

The total number of peptides identified for each protein by mass spectrometry was normalized by subtracting the number of peptides identified for the corresponding individual protein at the corresponding incubation time in the control (no nanoparticle) sample. Proteins with a peptide number of 2 or less were excluded from analysis as insignificant.[32]

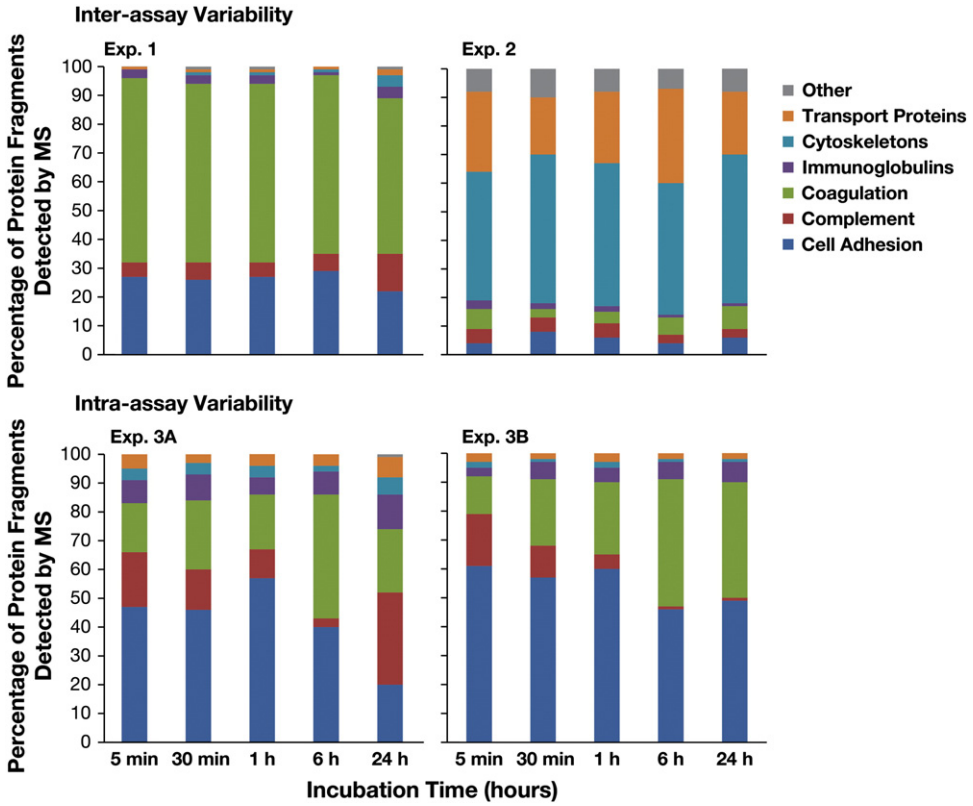

Figure 1. composition of protein corona over time. 30 nm gold colloids were incubated with pooled human plasma for 5 min, 30 min, 1 h, 6 h and 24 h. After several washes with PBS to remove excess plasma, the particle was pelleted and the particle pellet with bound proteins was analyzed by mass spectrometry. Proteins were grouped based on their function. Each bar shows the percentage of bound protein in each category for a given time point.

Complement activation

Platelet poor plasma (PPP) was prepared by centrifugation of freshly drawn whole blood for 10 min at 2500 × *g*. Activation of complement was assessed by the detection of the iC3b component of complement in test plasma samples using the commercial Quidel EIA kit (Santa Clara, CA, USA). Detailed protocol is provided in supplemental materials.

Plasma coagulation (PT, APTT and thrombin time)

To test whether gold colloids initiated plasma coagulation, normal human plasma pooled from 3 donors was treated with gold colloids and coagulation time was measured using the STArt4 coagulometer (Diagnostica Stago, Parsippany, NJ, USA). Detailed protocol is provided in supplemental materials.

Results

Physicochemical characterization

Physicochemical characterization included analysis of nanoparticle hydrodynamic size by dynamic light scattering (DLS), zeta potential by laser doppler velocimetry, and quantification of gold by inductively coupled plasma-mass spectrometry (ICP-MS). The data is summarized in Table 1. As expected, the hydrodynamic size increased and zeta potential shifted towards neutral as increasing molecular weights of PEG were applied to the particle surface. (Further details on the characterization can be found in the Supplemental Section.). Presence of equal amounts of PEG on the surface of PEGylated samples was confirmed by HPLC-CAD (data not shown).

Make-up of protein corona is consistent

For the purpose of the paper we will use "composition" to refer to the "make-up" of protein corona, i.e. the proteins, not the quantity of each individual protein. To evaluate inter-assay variability in protein corona composition, experiments were conducted at different times, each using plasma pooled from different donors. To assess intra-assay variability, a third experiment was conducted in which two independent sets of samples were run using the same pooled plasma. Regardless of the incubation time or plasma donors, the composition of the protein corona was fairly consistent. Proteins from the same functional categories – cell adhesion, complement, coagulation, immunoglobulins, cytoskeleton, and transport proteins – were identified in all experiments (Table 2). Furthermore, the majority of individual proteins identified within each functional category were also consistent between experiments.

In spite of consistency in the protein composition of the corona, the kinetics of protein binding varied greatly. Variability was observed at both the level of protein functional categories

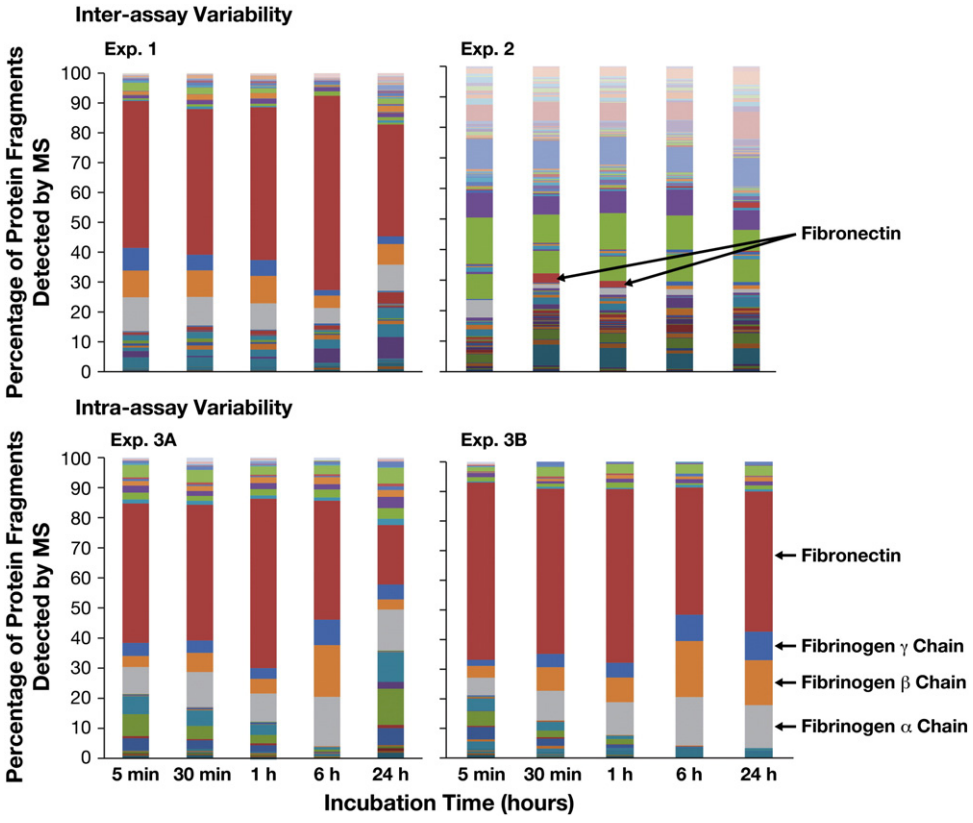

Figure 2. Kinetics of individual protein binding over time. 30 nm colloidal gold nanoparticles were incubated with pooled human plasma and proteins in the corona were identified by mass spectrometry. Presented is the summary of individual proteins identified over 5 min, 30 min, 1 h, 6 h and 24 h incubations.

(Figure 1) and at the level of individual proteins within each category (Figure 2). For example, in the inter-assay variability assessment, cell adhesion proteins made up the bulk of the corona in Experiment 1, while cytoskeleton proteins made up the bulk of the corona in Experiment 2. Across the various time points however, most protein levels remained fairly constant, generally fluctuating less than 10%. The largest exception to this was a 28% decrease in the number of cell adhesion protein between the 6 and 24 h time points of Experiment 1. In the intra-assay variability assessment, cell adhesion proteins comprised the bulk of the corona. Furthermore, there was significantly more variability in protein levels across the various time points. Cell adhesion proteins decreased 37% between 1 and 24 h, and complement proteins decreased 29% between 6 and 24 h in Experiment 3A. In Experiment 3B, coagulation proteins increased 27% between 5 min and 24 h, while complement and cell adhesion proteins both decreased approximately 15% across all time points (Figure 1).

Similarly, when analysis is done at the level of the individual protein, little consistency in kinetics was observed. For example, fibronectin was the most abundant protein in Experiment 1 at all time points, but was only detected in small quantities at 30 min and 1 h time points in Experiment 2. In the intra-assay variability assessment, fibronectin was the major protein in both experiments, but levels of other proteins varied between the replicates. For example, complement proteins were a significant component of the corona in Experiment 3A, but were almost nonexistent in Experiment 3B, and fibrinogen proteins comprised almost 40% of the corona in Experiment 3B, but only 22% in Experiment 3A at the 24 h time point.

The total amount of bound protein varied with each experiment. Again, there is little consistency in the kinetics of binding. Linear trend line analysis revealed a slight decrease in total protein in three of the four experiments over the entire timespan studied (Figure 3). However, three of the four experiments show an increase in total bound protein from the 6 h to 24 h time points. In Experiment 1, the 5 min time point has the most protein, and in Experiments 2, 3A and 3B the 30 min, 1 h and 6 h time points have the greatest protein content, respectively.

PEGylation decreases total protein, but does not dramatically change protein corona composition

The total amount of protein detected on the surface of gold nanoparticles was generally highest in uncoated gold colloids and decreased as the molecular weight of PEG increased (Figure 4). Also, the amount of bound protein generally decreased over time in all tested samples. The lowest amount of protein was detected on gold colloids coated with 20 kDa PEG; while some protein binding was observed at the 5 and 30 min time points, the amount of total protein was significantly diminished at the 6 h and 24 h time points (Figure 4). A decrease in total protein binding with

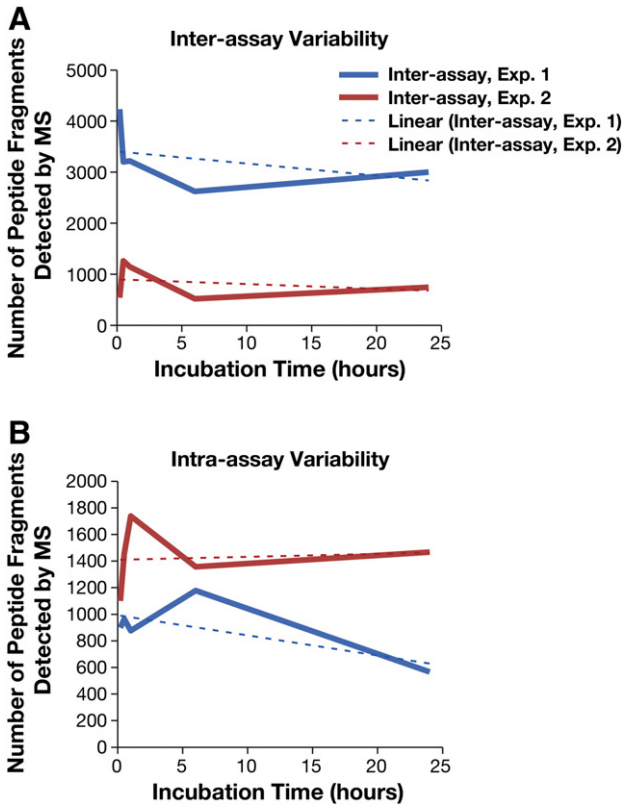

Figure 3. Kinetics of protein corona over time. 30 nm colloidal gold nanoparticles were incubated with pooled human plasma and proteins in the corona were identified by mass spectrometry. The total amount of bound protein identified over 5 min, 30 min, 1 h, 6 h and 24 h time points is shown. The linear trend line is shown as the color-coordinated dashed line, and was used to estimate the general trend in total bound protein between individual time points.

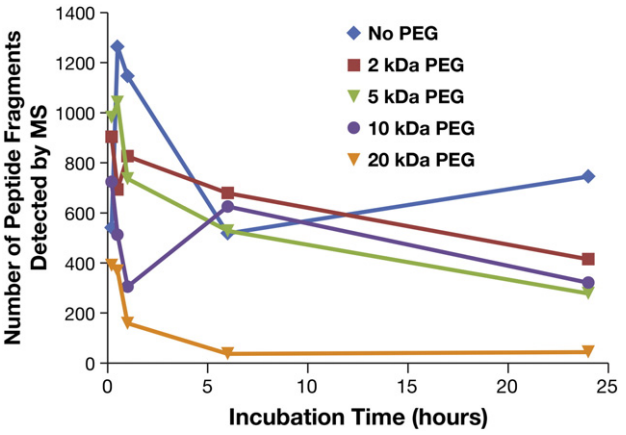

Figure 4. Kinetics of protein binding to gold colloids with various surface coatings. 30 nm core colloidal gold nanoparticles uncoated or coated with PEG of various molecular weights (2 kDa, 5 kDa, 10 kDa and 20 kDa) were incubated with pooled human plasma and proteins in the corona were identified by mass spectrometry. Presented is the total amount of bound protein identified over 5 min, 30 min, 1 h, 6 h and 24 h incubation periods.

increased PEG molecular weight was also confirmed by 1D PAGE with densitometry analysis (see Supplemental Section).

In spite of the differences noted in the amount of total bound protein, the protein composition of the corona was not dramatically affected. Proteins detected in the corona of 30 nm uncoated gold colloids were also detected in corona of PEGylated gold nanoparticles (Table 3). The noted exceptions to this were extracellular matrix proteins, which were undetected in all PEGylated samples, and immunoglobulins, which were undetected in the corona of 20 kDa PEGylated gold colloids (Table 3, red font).

Plasma coagulation and complement system are unaffected

Since both complement components and plasma coagulation factors were among the most abundant proteins identified in the corona, we assessed whether the binding of these proteins to the nanoparticle surface would alter their physiological function. Complement and plasma coagulation functions were assessed *in vitro* using normal human plasma pooled from several donors. Nanoparticles *per se* did not activate plasma coagulation (Figure 5, *A*) and did not activate the complement system (Figure 6, *A*). Interestingly, low activation of the alternative pathway was detected as seen by weak elevation of Bb levels (Figure 6, *A*, Bb bar). However, this activation was not strong enough to proceed along the cascade to generate substantial levels of C3 split products (Figure 6, *A*, iC3b bar). Cobra venom factor (CVF) activates complement through the alternative pathway, and was not expected to generate a positive response in C4d assay. The assay performance was monitored by quality controls supplied with the kit.

We also assessed whether nanoparticles would affect plasma coagulation or complement functions initiated by a known activator. To assess particle effects on plasma coagulation, plasma was pretreated with gold colloids, and after nanoparticles and nanoparticle-bound proteins were removed, plasma was then subjected to a known plasma coagulation initiator. Gold nanoparticles did not interfere with plasma coagulation time in either PT or APTT assays with known initiators (Figure 5, *B*, compare UT bars with H_2O [vehicle] and 30 nm Au-NP bars). Plasma was also pre-treated with two concentrations of thrombin, which is known to deplete fibrinogen, one of the major components of the protein corona of gold nanoparticles. If the depletion of fibrinogen as a result of nanoparticle binding is physiologically significant, we expected to see a delay in plasma coagulation. Plasma coagulation in samples pre-treated with the standard concentration (0.15 NIH U/mL) of thrombin was delayed in both PT and APTT assays, as was expected (Figure 5, *B* APTT and PT panels, compare D1 bars with UT bars). However, when a lower concentration (0.015NIH U/mL) of thrombin (to assess potentially lower potency of the gold nanoparticles) was used, a slight acceleration of plasma coagulation was observed (compare D10 bars with UT bars on Figure 5, *B*).

To assess effects on the complement system, plasma was incubated with gold colloids or water (vehicle control) for 30 min; after centrifugation to remove the gold colloids and any complement proteins bound to the particles, plasma supernatants of each sample were split into 3 parts and tested against PBS (negative control), Taxol (nanoparticle positive control) and

Table 3
Individual proteins identified by mass spectrometry in the protein corona surrounding 30 nm core gold colloids with various surface coatings.

Protein category	un PEGylated	2 kDa PEG	5 kDa PEG	10 kDa PEG	20 kDa PEG
Cell adhesion	Fibronectin, vitronectin, thrombospondin, integrins, beta parvin, vasodilator-stimulated phosphoprotein	Fibronectin, vitronectin, thrombospondin, integrins, beta parvin, vasodilator-stimulated phosphoprotein	Fibronectin, vitronectin, thrombospondin, integrins, beta parvin, vasodilator-stimulated phosphoprotein	Fibronectin, vitronectin, thrombospondin, integrins, beta parvin, vasodilator-stimulated phosphoprotein	Fibronectin, vitronectin, thrombospondin, integrins, beta parvin, vasodilator-stimulated phosphoprotein
Complement	C1q, C3, C4a	C1q, C3, C4a	C1q, C3, C4a	C1q, C3, C4a	C1q, C3, C4a
Coagulation	Fibrinogen, FXIII, pGP, kininogen, CD9, histidine-rich glycoprotein, multimerin	Fibrinogen, FXIII, pGP, kininogen, CD9, histidine-rich glycoprotein, multimerin	Fibrinogen, FXIII, pGP, kininogen, CD9, histidine-rich 2glycoprotein, multimerin	Fibrinogen, FXIII, pGP, kininogen, CD9, histidine-rich glycoprotein, multimerin	Fibrinogen, FXIII, pGP, kininogen, CD9, histidine-rich glycoprotein, multimerin
Immunoglobulins	IgG and IgM light chains	IgG and IgM light chains	IgG and IgM light chains	IgG and IgM light chains	ND
Cytoskeleton	Actin, myosin, tropomyosin, tubulin, filamin, gelsolin, F-actin, vinculin, coronin, cofilin, transgelin, ezrin, zyxin, profiling, caldesmon, PDZ and LIM domain protein 1, multimerin	Actin, myosin, tropomyosin, tubulin, filamin, gelsolin, F-actin, vinculin, coronin, cofilin, transgelin, ezrin, zyxin, profiling, caldesmon, PDZ and LIM domain protein 1, multimerin	Actin, myosin, tropomyosin, tubulin, filamin, gelsolin, F-actin, vinculin, coronin, cofilin, transgelin, ezrin, zyxin, profiling, caldesmon, PDZ and LIM domain protein 1, multimerin	Actin, myosin, tropomyosin, tubulin, filamin, gelsolin, F-actin, vinculin, coronin, cofilin, transgelin, ezrin, zyxin, profiling, caldesmon, PDZ and LIM domain protein 1, multimerin	Actin, myosin, tropomyosin, tubulin, filamin, gelsolin, F-actin, vinculin, coronin, cofilin, transgelin, ezrin, zyxin, profiling, caldesmon, PDZ and LIM domain protein 1, multimerin
Transport	Albumin, anion transport protein, Apo C, Apo E, Apo A, Apo J, hemoglobin, 78kD glucose regulated protein	Albumin, anion transport protein, Apo C, Apo E, Apo A, Apo J, hemoglobin, 78kD glucose regulated protein	Albumin, anion transport protein, Apo C, Apo E, Apo A, Apo J, hemoglobin, 78kD glucose regulated protein	Albumin, anion transport protein, Apo C, Apo E, Apo A, Apo J, hemoglobin, 78kD glucose regulated protein	Albumin, anion transport protein, Apo C, Apo E, Apo A, Apo J, hemoglobin, 78kD glucose regulated protein
Extracellular matrix	Tenascin	ND	ND	ND	ND
Cellular signal transduction	Ras, Rab, 14-3-3 protein Z, protein S100-A9, fermitin	Ras, Rab, 14-3-3 protein Z, protein S100-A9, fermitin	Ras, Rab, 14-3-3 protein Z, protein S100-A9, fermitin	Ras, Rab, 14-3-3 protein Z, protein S100-A9, fermitin	Ras, Rab, 14-3-3 protein Z, protein S100-A9, fermitin
Enzymes	Glyceraldehyde phosphate dehydrogenase, adenylyl cyclase, aldolase, isocitrate dehydrogenase, protein-disulfide isomerase, triosephosphate isomerase, ATP synthase, lactade dehydrogenase, enolase, pyruvate kinase, frusctose-biphosphate aldolase, peptidyl-prolyl cis-trans isomerase, carbonic anhydrase, glyceraldehyde-3 phosphate dehydrogenase	Glyceraldehyde phosphate dehydrogenase, adenylyl cyclase, aldolase, isocitrate dehydrogenase, protein-disulfide isomerase, triosephosphate isomerase, ATP synthase, lactade dehydrogenase, enolase, pyruvate kinase, frusctose-biphosphate aldolase, peptidyl-prolyl cis-trans isomerase, carbonic anhydrase, glyceraldehyde-3 phosphate dehydrogenase	Glyceraldehyde phosphate dehydrogenase, adenylyl cyclase, aldolase, isocitrate dehydrogenase, protein-disulfide isomerase, triosephosphate isomerase, ATP synthase, lactade dehydrogenase, enolase, pyruvate kinase, frusctose-biphosphate aldolase, peptidyl-prolyl cis-trans isomerase, carbonic anhydrase, glyceraldehyde-3 phosphate dehydrogenase	Glyceraldehyde phosphate dehydrogenase, adenylyl cyclase, aldolase, isocitrate dehydrogenase, protein-disulfide isomerase, triosephosphate isomerase, ATP synthase, lactade dehydrogenase, enolase, pyruvate kinase, frusctose-biphosphate aldolase, peptidyl-prolyl cis-trans isomerase, carbonic anhydrase, glyceraldehyde-3 phosphate dehydrogenase	Glyceraldehyde phosphate dehydrogenase, adenylyl cyclase, aldolase, isocitrate dehydrogenase, protein-disulfide isomerase, triosephosphate isomerase, ATP synthase, lactade dehydrogenase, enolase, pyruvate kinase, frusctose-biphosphate aldolase, peptidyl-prolyl cis-trans isomerase, carbonic anhydrase, glyceraldehyde-3 phosphate dehydrogenase
Stress-response	Heat shock protein, serum-deprivation protein	Heat shock protein, serum-deprivation protein	Heat shock protein, serum-deprivation protein	Heat shock protein, serum-deprivation protein	Heat shock protein, serum-deprivation protein
Other	Histone H4, Hermansky-Pudlock syndrome 1 protein, thymosin, erythrocyte band 7 integral membrane protein	Histone H4, Hermansky-Pudlock syndrome 1 protein, thymosin, erythrocyte band 7 integral membrane protein	Histone H4, Hermansky-Pudlock syndrome 1 protein, thymosin, erythrocyte band 7 integral membrane protein	Histone H4, Hermansky-Pudlock syndrome 1 protein, thymosin, erythrocyte band 7 integral membrane protein	Histone H4, Hermansky-Pudlock syndrome 1 protein, thymosin, erythrocyte band 7 integral membrane protein

30 nm colloidal gold nanoparticles, un-PEGylated or coated with 2 kDa, 5 kDa, 10 kDa or 20 kDa PEG, were incubated with pooled human plasma and proteins in the corona were identified by mass spectrometry. Below is the summary of all proteins identified in each time point studied (5 min, 30 min, 1 h, 6 h and 24 h), grouped by their function. ND - not detected.

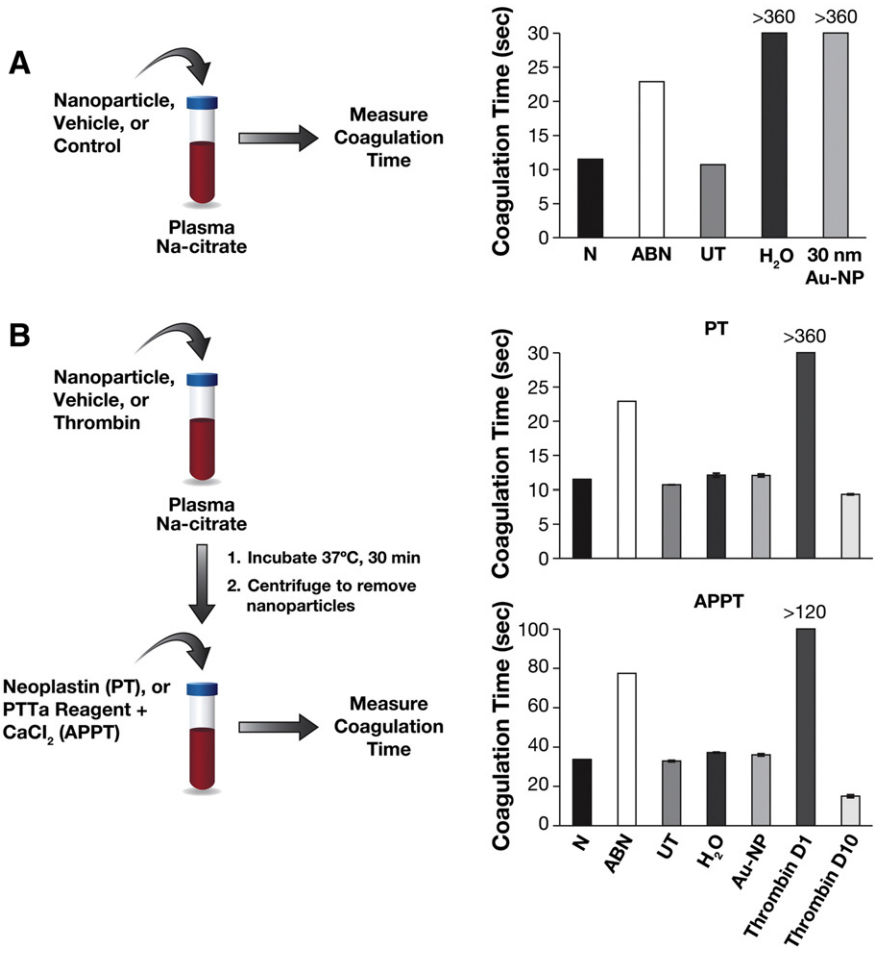

Figure 5. Nanoparticles and plasma coagulation. (**A**) 30 nm colloidal gold nanoparticles were studied *in vitro* to evaluate their pro-coagulant properties. Coagulation in normal control (N), abnormal control (ABN) and untreated healthy donor plasma (UT) was initiated by the addition of Neoplastin reagent. Water (H_2O) and gold colloids (30 nm Au-NP) were also tested for initiation of coagulation in samples of untreated healthy donor plasma. (**B**) Pooled human plasma was either untreated (UT) or treated with 30 nm gold colloids (Au-NP), high concentration (0.15NIHU/mL) of thrombin (thrombin D1) or low (0.015NIH U/mL) concentration of thrombin (thrombin D10) for 30 min at 37 °C. Plasma coagulation was initiated in all samples by the addition of Neoplastin reagent (PT) or PTTa reagent and calcium chloride (APPT); >360 refers to the absence of detectable coagulation within 6 min; each bar shows the mean of duplicate results (% CV <5).

CVF (positive control). Gold nanoparticles did not affect complement activation by Taxol and CVF (Figure 6, *B*).

Discussion

Gold colloids are increasingly used for drug delivery, and the role of their surface coating in biodistribution has been previously established[21,23,27]. However, the composition of the protein corona, and its role in the hematocompatibility of gold colloids has not been fully explored. Therefore, we examined the kinetics of plasma protein binding to the surface of citrate stabilized gold colloids with a nominal size of 30 nm, as well as derivatives bearing PEG coatings of different molecular weights (2 kDa, 5 kDa, 10 kDa and 20 kDa). To avoid variability in the protein repertoire due to storage conditions and inter-donor variability, we have used fresh whole blood drawn from at least 3 healthy donor volunteers, and processed within 1 hour to obtain plasma; the plasma was then pooled and used immediately for each experiment. To avoid donor-specific bias in repeated experiments, pooled plasma from different donors was used for each experiment. Our data demonstrate that the protein composition of the corona is fairly consistent in both inter- and intra-assay variability assessments (Table 2), and is also consistent with our previous study using 2D PAGE to separate and identify nanoparticle bound proteins.[7] However, the amount of bound protein and the kinetics of binding varied between experiments (Figures 1–3).

The so called “Vroman’s effect”, initially reported in 1962 and related to competitive adsorption of plasma proteins to surfaces with different hydrophobicity, was expected to apply to engineered nanomaterials.[33] Several research groups have attempted to verify this hypothesis. Vroman’s effect was confirmed for polymeric and solid lipid nanoparticles, while studies with oil-in-water emulsions and iron oxide nanoparticles concluded there was no displacement of previously adsorbed

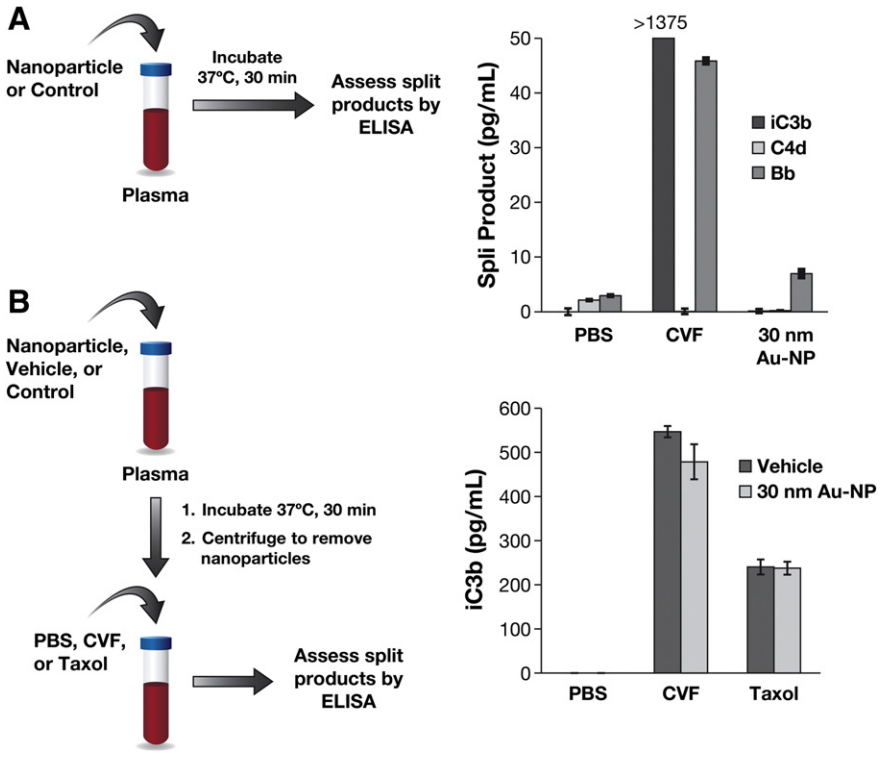

Figure 6. Nanoparticles and complement activation. (**A**) 30 nm colloidal gold nanoparticles were studied *in vitro* to evaluate their ability to activate the human complement system. Pooled normal human plasma was treated with PBS, cobra venom factor (CVF) or nanoparticles for 30 min at 37 °C, and complement split products iC3b, C4d and Bb were measured by ELISA. (**B**) Pooled human plasma was treated with 30 nm gold colloids (30 nm Au-NP) or vehicle (water) for 30 min at 37 °C. Following incubation, plasma was spun down to remove particles, and supernatants were treated with PBS, CVF or Taxol. Complement split products were monitored by ELISA. Each bar shows the mean ± SD (N = 3).

proteins.[12,34–36] Results of our data are in agreement with that reported for nanoemulsions and iron oxide particles, i.e. there is no competitive displacement; proteins detected at 5 min are also detected at 24 h time point (Figure 1). One possible explanation for this difference could be that gold colloids are more similar to iron oxide nanoparticles in terms of lower hydrophobicity than that of solid lipid nanoparticles. Another possible explanation is that the studies suggesting the existence of Vroman's effect for nanomaterials used diluted plasma, which changes the ratio between the nanoparticle and certain plasma proteins. Lastly, these studies all use different incubation periods for protein binding. According to Vroman et al, displacement takes place within the first seconds[33]; the shortest incubation time in our study was 5 min.

Another interesting observation from our study is that regardless of the method (2D PAGE followed by mass spectrometry[7] vs. direct processing for MS analysis), and in spite of the fact that we used plasma from different donors for each experiment, the functional categories of proteins detected in the protein corona are consistent (Figure 1, Table 1). It is our understanding that all previous studies used the same plasma or animal serum (individual or pooled) for experiments. Since our data suggest that protein binding is not specific, prediction of toxicities based on the protein corona determined from a single donor or single pool of plasma is less likely to be accurate. It is also worthwhile to note the composition of the protein corona may be affected based on the matrix used in the study. For example, fibrinogen is abundant in plasma but not in serum; absence of this protein in serum will certainly influence the composition of the corona.

Nanoparticle surface modification with PEG is widely recognized as an efficient means of protection from opsonization and subsequent immune recognition.[23] Here we studied how nanoparticle surface modification with PEG of various molecular weights influences the kinetics of protein binding over 24 hours and the composition of the protein corona. During the first 5 minutes of incubation there was no clear trend in the total protein binding between unPEGylated gold and its PEGylated counterparts (Figure 4). A likely explanation for this observation is difference in incubation temperature. All plasma samples were handled at room temperature to avoid spontaneous complement activation; incubation on ice was not used as it can alter the plasma proteome by triggering activation of the coagulation cascade. After sample preparation, incubation was performed at 37 °C; however, it takes about 5 min for the sample to equilibrate to 37 °C. Thus, during the initial 5 min of incubation sample was likely subjected to a range of temperatures from 22 °C to 37 °C. After 30 and 60 minutes incubation there was a clear difference in total protein binding between the samples. Total protein in the corona generally decreased with increased molecular weight of PEG. At the 6 and 24 h time points there was no significant difference in total protein binding between

gold colloids with 2 kDa, 5 kDa and 10 kDa PEG. At time points between 30 min and 24 h there was dramatic difference in total bound protein between the unPEGylated gold and gold coated with 20 kDa PEG (Figure 4). This data is in agreement with biological studies showing a dramatic difference in opsonization and biodistribution to MPS organs of animals injected with 30 nm gold colloids with and without 20 kDa PEG.[23] Interestingly, in spite of the difference in total protein binding between unPEGylated and PEGylated gold colloids, the composition of protein corona did not change dramatically (Table 3). All proteins detected in the corona of the unPEGylated 30 nm gold colloids were also detected, although at much lower quantity, in the corona of the PEGylated nanoparticles with two exceptions: 1) extracellular matrix proteins were not detected on all PEGylated particles, and 2) immunoglobulins were not detected on gold colloids coated with 20 kDa PEG. This data is consistent with that reported by Gref et al. who also detected a decrease in the total amount of protein binding but no substantial change in the composition of the protein corona for solid lipid nanoparticles (SLN).[37] Similar to our study, light chain immunoglobulins were not detected in the corona of PEGylated SLN in contrast to their unPEGylated counterparts.[37] This phenomenon seems to be common for nanoparticles of different composition and size (our study used small [<100 nm] anionic core particles, while Gref et al used large [>200 nm] cationic core particles) when coated with large PEG moieties (20 kDa in our study and 45 kDa in the SLN study). We hypothesize the mechanism for immunoglobulin exclusion may be related to steric hindrance. The polymer coating does not cover the entire particle surface, leaving some sites for capture of proteins; however, due to their size and conformation not all proteins can reach the particle surface, which in turn leads to exclusion of these proteins.

To understand whether knowing the protein corona composition could be used to predict hematological toxicity, we performed routine hematology tests focusing on complement and coagulation, since proteins representing these two systems were consistently abundant in the corona of these gold nanoparticles. Fibrinogen binding to gold colloids does not change the function of this protein. Neither induction of plasma coagulation by particles *per se,* nor disturbance of plasma coagulation induced by known agonists of both extrinsic and intrinsic pathways was detected in plasma pretreated with gold nanoparticles (Figure 5). We also showed that gold colloids do not activate the complement system, and that activation of complement by some known stimuli, such as CVF and Taxol, was unaffected (Figure 6). These data suggest that binding of complement proteins and proteins involved in plasma coagulation to the surface of gold colloids does not lead to the depletion of these proteins to levels which would become insufficient for normal function. Our data is consistent with previous studies utilizing carbon nanotubes and functionalized gold and metal oxide nanoparticles, reporting that binding of the complement protein or fibrinogen *per se* does not always cause activation of the protein and/or a change in the protein function.[14–16,38–40] Since both complement and fibrinogen are highly abundant proteins in plasma, the particle concentration required to deplete these proteins to a level affecting their function must be very high. Achieving such high concentration *in vitro* is possible for some but not all nanoparticles. While protein concentration is constant under *in vitro* conditions, it is dynamic *in vivo* due to homeostasis. Thus, a particle concentration affecting protein function *in vivo* presumably should be even higher. This further emphasizes the importance of hematocompatibility tests in establishing nanoparticle safety profiles and suggests that detection and identification of the composition of a nanoparticle's protein corona cannot reliably serve this function.

In summary, we demonstrated that surface properties (i.e. PEGylation) of colloidal gold nanoparticles determine the amount of total bound protein, but only slightly affect the composition of the protein corona. The overall protein corona composition fluctuates with time but is generally consistent between experiments utilizing plasma from different donors. Identification of proteins in the corona cannot be used to substitute relevant biocompatibility tests, as binding *per se* does not directly correlate to a change in protein function.

Appendix A. Supplementary data

Supplementary data to this article can be found online at http://dx.doi.org/10.1016/j.nano.2014.01.009.

References

1. Treuel L, Nienhaus GU. Nanoparticle interaction with plasma proteins as it relates to biodistribution. In: Dobrovolskaia MA, McNeil SE, editors. *Handbook of immunological properties of engineered nanomaterials. 1*. Singapore: World Scientific Publishing Co. Pte. Ltd.; 2013. p. 151-64.
2. Cedervall T, Lynch I, Foy M, Berggard T, Donnelly SC, Cagney G, et al. Detailed identification of plasma proteins adsorbed on copolymer nanoparticles. *Angew Chem Int Ed Engl* 2007;**46**:5754-6.
3. Goppert TM, Muller RH. Polysorbate-stabilized solid lipid nanoparticles as colloidal carriers for intravenous targeting of drugs to the brain: comparison of plasma protein adsorption patterns. *J Drug Target* 2005;**13**:179-87.
4. Michaelis K, Hoffmann MM, Dreis S, Herbert E, Alyautdin RN, Michaelis M, et al. Covalent linkage of apolipoprotein e to albumin nanoparticles strongly enhances drug transport into the brain. *J Pharmacol Exp Ther* 2006;**317**:1246-53.
5. Nagayama S, Ogawara K, Minato K, Fukuoka Y, Takakura Y, Hashida M, et al. Fetuin mediates hepatic uptake of negatively charged nanoparticles via scavenger receptor. *Int J Pharm* 2007;**329**:192-8.
6. Zensi A, Begley D, Pontikis C, Legros C, Mihoreanu L, Wagner S, et al. Albumin nanoparticles targeted with Apo E enter the CNS by transcytosis and are delivered to neurones. *J Control Release* 2009;**137**:78-86.
7. Dobrovolskaia MA, Patri AK, Zheng J, Clogston JD, Ayub N, Aggarwal P, et al. Interaction of colloidal gold nanoparticles with human blood: effects on particle size and analysis of plasma protein binding profiles. *Nanomedicine* 2009;**5**:106-17.
8. Lundqvist M, Stigler J, Cedervall T, Berggard T, Flanagan MB, Lynch I, et al. The evolution of the protein corona around nanoparticles: a test study. *ACS Nano* 2011;**5**:7503-9.
9. Casals E, Puntes VF. Inorganic nanoparticle biomolecular corona: formation, evolution and biological impact. *Nanomedicine (Lond)* 2012;**7**:1917-30.
10. Gebauer JS, Malissek M, Simon S, Knauer SK, Maskos M, Stauber RH, et al. Impact of the nanoparticle-protein corona on colloidal stability and protein structure. *Langmuir* 2012;**28**:9673-9.

11. Hoshino Y, Nakamoto M, Miura Y. Control of protein-binding kinetics on synthetic polymer nanoparticles by tuning flexibility and inducing conformation changes of polymer chains. *J Am Chem Soc* 2012;**134**:15209-12.
12. Jansch M, Stumpf P, Graf C, Ruhl E, Muller RH. Adsorption kinetics of plasma proteins on ultrasmall superparamagnetic iron oxide (USPIO) nanoparticles. *Int J Pharm* 2012;**428**:125-33.
13. Milani S, Bombelli FB, Pitek AS, Dawson KA, Radler J. Reversible versus irreversible binding of transferrin to polystyrene nanoparticles: soft and hard corona. *ACS Nano* 2012;**6**:2532-41.
14. Deng ZJ, Liang M, Toth I, Monteiro M, Minchin RF. Plasma protein binding of positively and negatively charged polymer-coated gold nanoparticles elicits different biological responses. *Nanotoxicology* 2013;**7**:314-22.
15. Deng ZJ, Liang M, Toth I, Monteiro MJ, Minchin RF. Molecular interaction of poly(acrylic acid) gold nanoparticles with human fibrinogen. *ACS Nano* 2012;**6**:8962-9.
16. Deng ZJ, Mortimer G, Schiller T, Musumeci A, Martin D, Minchin RF. Differential plasma protein binding to metal oxide nanoparticles. *Nanotechnology* 2009;**20**:455101.
17. Lundqvist M, Stigler J, Elia G, Lynch I, Cedervall T, Dawson KA. Nanoparticle size and surface properties determine the protein corona with possible implications for biological impacts. *Proc Natl Acad Sci U S A* 2008;**105**:14265-70.
18. Monopoli MP, Aberg C, Salvati A, Dawson KA. Biomolecular coronas provide the biological identity of nanosized materials. *Nat Nanotechnol* 2012;**7**:779-86.
19. Walczyk D, Bombelli FB, Monopoli MP, Lynch I, Dawson KA. What the cell "sees" in bionanoscience. *J Am Chem Soc* 2010;**132**:5761-8.
20. Mahmoudi M, Saeedi-Eslami SN, Shokrgozar MA, Azadmanesh K, Hassanlou M, Kalhor HR, et al. Cell "vision": complementary factor of protein corona in nanotoxicology. *Nanoscale* 2012;**4**:5461-8.
21. Hainfeld JF, Slatkin DN, Focella TM, Smilowitz HM. Gold nanoparticles: a new X-ray contrast agent. *Br J Radiol* 2006;**79**:248-53.
22. Liu J, Lu Y. Colorimetric biosensors based on DNAzyme-assembled gold nanoparticles. *J Fluoresc* 2004;**14**:343-54.
23. Paciotti GF, Myer L, Weinreich D, Goia D, Pavel N, McLaughlin RE, et al. Colloidal gold: a novel nanoparticle vector for tumor directed drug delivery. *Drug Deliv* 2004;**11**:169-83.
24. Thaxton CS, Georganopoulou DG, Mirkin CA. Gold nanoparticle probes for the detection of nucleic acid targets. *Clin Chim Acta* 2006;**363**:120-6.
25. Diluzio NR, Zilversmit DB. Influence of exogenous proteins on blood clearance and tissue distribution of colloidal gold. *Am J Physiol* 1955;**180**:563-5.
26. Goel R, Shah N, Visaria R, Paciotti GF, Bischof JC. Biodistribution of TNF-alpha-coated gold nanoparticles in an in vivo model system. *Nanomedicine (Lond)* 2009;**4**:401-10.
27. Rygard J. Mechanism of blood clearance of colloidal gold in mice. An atoxic clinical investigation using activation analysis. *Acta Radiol Suppl* 1971;**308**:1-240.
28. Terentyuk GS, Maslyakova GN, Suleymanova LV, Khlebtsov BN, Kogan BY, Akchurin GG, et al. Circulation and distribution of gold nanoparticles and induced alterations of tissue morphology at intravenous particle delivery. *J Biophotonics* 2009;**2**:292-302.
29. Kah JC, Wong KY, Neoh KG, Song JH, Fu JW, Mhaisalkar S, et al. Critical parameters in the pegylation of gold nanoshells for biomedical applications: an in vitro macrophage study. *J Drug Target* 2009;**17**:181-93.
30. O'Neal DP, Hirsch LR, Halas NJ, Payne JD, West JL. Photo-thermal tumor ablation in mice using near infrared-absorbing nanoparticles. *Cancer Lett* 2004;**209**:171-6.
31. Mirkin CA, Lytton-Jean AKR, Hurst SJ, inventorsMaximizing Oligonucleotide Loading on Gold Nanoparticle. USAUS Patent US2010/0099858, publication date November 9, 2009.
32. Issaq HJ, Chan KC, Blonder J, Ye X, Veenstra TD. Separation, detection and quantitation of peptides by liquid chromatography and capillary electrochromatography. *J Chromatogr A* 2009;**1216**:1825-37.
33. Vroman L, Adams AL, Fischer GC, Munoz PC. Interaction of high molecular weight kininogen, factor XII, and fibrinogen in plasma at interfaces. *Blood* 1980;**55**:156-9.
34. Blunk T, Luck M, Calvor A, Hochstrasser DF, Sanchez JC, Muller BW, et al. Kinetics of plasma protein adsorption on model particles for controlled drug delivery and drug targetting. *Eur J Pharm Biopharm* 1996;**42**:262-8.
35. Goppert TM, Muller RH. Adsorption kinetics of plasma proteins on solid lipid nanoparticles for drug targeting. *Int J Pharm* 2005;**302**:172-86.
36. Harnisch S, Muller RH. Adsorption kinetics of plasma proteins on oil-in-water emulsions for parenteral nutrition. *Eur J Pharm Biopharm* 2000;**49**:41-6.
37. Gref R, Luck M, Quellec P, Marchand M, Dellacherie E, Harnisch S, et al. 'Stealth' corona-core nanoparticles surface modified by polyethylene glycol (PEG): influences of the corona (PEG chain length and surface density) and of the core composition on phagocytic uptake and plasma protein adsorption. *Colloids Surf B: Biointerfaces* 2000;**18**:301-13.
38. Deng ZJ, Liang M, Monteiro M, Toth I, Minchin RF. Nanoparticle-induced unfolding of fibrinogen promotes Mac-1 receptor activation and inflammation. *Nat Nanotechnol* 2011;**6**:39-44.
39. Salvador-Morales C, Basiuk EV, Basiuk VA, Green ML, Sim RB. Effects of covalent functionalization on the biocompatibility characteristics of multi-walled carbon nanotubes. *J Nanosci Nanotechnol* 2008;**8**:2347-56.
40. Salvador-Morales C, Flahaut E, Sim E, Sloan J, Green ML, Sim RB. Complement activation and protein adsorption by carbon nanotubes. *Mol Immunol* 2006;**43**:193-201.